URSI GASS 2021, Rome, Italy, 28 August - 4 September 2021

Anisotropic Waveform-Selective Metasurfaces

Haruki Homma [(1)], Jiyeon Lee[(2)], and Hiroki Wakatsuchi[(1,3)]
(1) Department of Electrical and Mechanical Engineering, Graduate School of Engineering,
Nagoya Institute of Technology, Nagoya, Aichi, 466-8555, Japan; e-mail: wakatsuchi.hiroki@nitech.ac.jp
(2) Electrical and Computer Engineering Department, University of California at San Diego,
San Diego, CA 92093-0407, USA; email: y0l001@ucsd.edu
(3) Precursory Research for Embryonic Science and Technology (PRESTO),
Japan Science and Technology Agency (JST), Saitama 332-0012, Japan

Abstract

In recent years, circuit-based metasurfaces containing diode bridges were reported to selectively respond to a particular incident wave among others even at the same frequency by sensing waveforms, namely, pulse widths. In this study, we study such waveform-selective metasurfaces but with an anisotropy to achieve beam shifting or guiding of a particular waveform only. These results are expected to give us an additional degree of freedom to address existing electromagnetic issues including suppression of electromagnetic noise/interference.

1 Introduction

Metasurfaces are known as artificially engineered periodic/aperiodic subwavelength surfaces that enable us to design a wide range of electromagnetic properties [1-3]. For instance, a surface wave entering a metasurface can be reflected or transmitted depending on the surface impedance. The concept of this wave propagation can be extended from 1D to 2D by introducing an anisotropy into the surface impedance of a metasurface [4-6]. In this way, metasurfaces can have different surface impedances along two orthogonal axes, which potentially enables us to guide a surface wave to only one of the axes. Such a capability is useful in, for instance, avoidance of scattering objects to maintain wireless communications between antennas. However, usually anisotropic metasurfaces have static properties unless, for instance, an active mechanism is introduced, which means that any wave propagating on the surfaces is guided in the same manner. In more recent years, circuit-based metasurfaces were demonstrated to distinguish different waves even at the same frequency depending on their waveforms, namely, on their pulse widths [7-12]. Such waveform-selective metasurfaces were also exploited as a cloaking device and a signal-processing cavity [10-11]. However, waveform-selective metasurfaces were so far reported to control the absorption, reflection, and transmission of a surface wave along one direction only [7, 8]. In this study, we therefore introduce an anisotropy into waveform-selective metasurfaces to extend the concept of waveform selectivity and to provide a more freedom to guide surface waves. These anisotropic waveform-selective metasurfaces make it possible to send a particular signal to a receiver, while reducing its scattering for other types of waveforms at the same frequency.

2 Theory

Although mode details are reported in past studies [7, 8], waveform-selective mechanisms can be understood as follows. Firstly, an incident surface wave induces electric charges on conductors of a metasurface. At a resonant frequency, the metasurface strongly resonates and exhibits strong electric field in gaps between conductor edges like other ordinary metasurfaces. In the case of the waveform-selective metasurface, however, each conductor gap is connected by a set of four diodes to convert the frequency of the incoming energy into an infinite set of frequencies. Importantly, most energy is converted to zero frequency here, as the diodes play a role of a diode bridge to fully rectify the incident waveform (i.e., the rectified waveform varies in proportion to almost the absolute value of a sine function, namely, to |sin|). In addition, the energy entering into the diode bridge is controlled by other circuit components such as inductors and resistors. Other types of waveform-selective metasurfaces are also reported in the literature [7-9]. This study used ANSYS Electromagnetics Desktop (2020 R2) to numerically test several types of metasurfaces below.

3 Results

3.1 Anisotropic Metasurfaces

Firstly, we tested simple anisotropic metasurfaces. Fig. 1 shows surface impedances of different metasurfaces. As seen in this figure, if square patches were paired as rectangular patches, a surface impedance increased compared to a square case or even the impedance along another axis (compare the red curve to the two blue curves between 3.0 and 3.4 GHz of Fig. 1). Therefore, the propagation of a surface can be bent along the direction of a lower surface impedance. In Fig. 2a, where an isotropic metasurface composed of square patches was deployed in front of an antenna, a surface wave propagated widely but mostly downwards. In contrast, the propagation of a surface wave was clearly bent along the direction of the bottom left in Fig. 2b. Along this direction, the metasurface used in Fig. 2b had a relatively lower surface impedance. These results demonstrate that the use of anisotropic surface impedances makes it possible to guide an incoming surface wave to a particular direction.

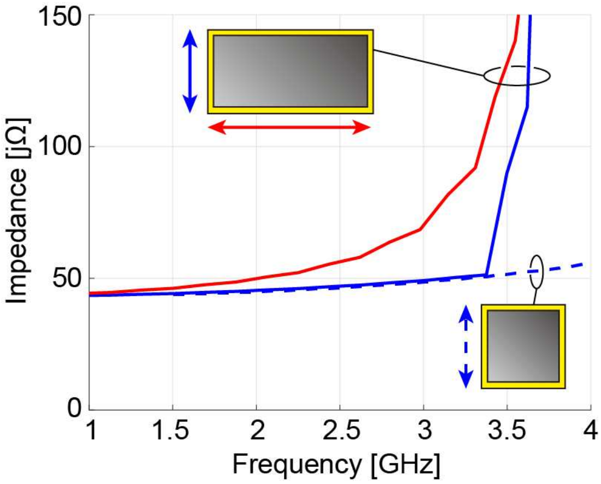

Figure 1. Surface impedances of metasurfaces. The insets represent the periodic unit cells of the metasurfaces used. The rectangular patches were simulated for two orthgonal axes due to its asymmetric conducting geometry (see the blue and red solid arrows).

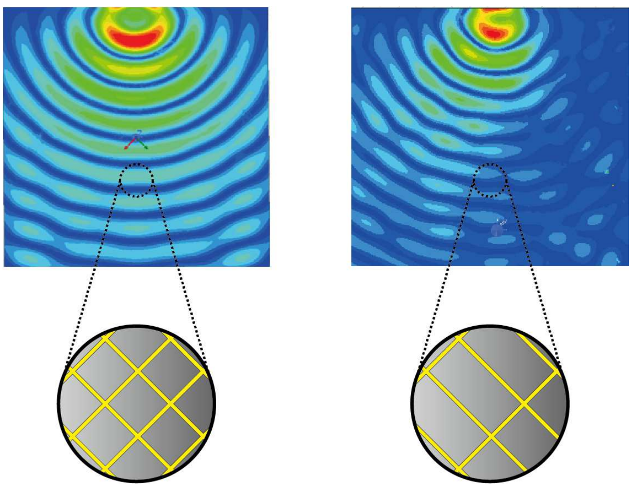

(a) (b)

Figure 2. Electric field distributions of (a) an isotropic metasurface and (b) an anisotropic metasurface. An antenna was deployed at the top center of each simulation space.

3.2 Nonlinear Anisotropic Metasurfaces

Before introducing an anisotropy into waveform-selective metasurfaces, we tested another simplified case where square conducting patches were connected or disconnected in response to the power level of an incoming surface wave. This was achieved by connecting conductor edges by paired diodes (Fig. 3a). However, since simulating a large number of periodic unit cells of the nonlinear anisotropic metasurface required extremely strong computational effort, we tested only one metasurface line inside a TEM waveguide to see how the transmission changed (Fig. 4). Simulation results show that the metasurface strongly transmitted a surface wave of 0 dBm within the frequency range simulated between 2 and 5 GHz (Fig. 5). This is because the paired diodes did not electrically connect conducting patches yet. By increasing the input power to 40 dBm, however, the diodes used were fully turned on. As a result, patches were connected to effectively form rectangular patches, preventing the propagation of a surface wave near 4 GHz. These results indicate that an isotropic metasurface can switch to an anisotropic metasurface by connecting square patches as seen in Figs. 1 and 2.

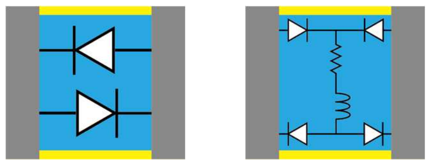

(a) (b)

Figure 3. The circuit configurations used for (a) a nonlinear metasurface and (b) a waveform-selective metasurface. These circuits were deployed between conducting patches of Fig. 4.

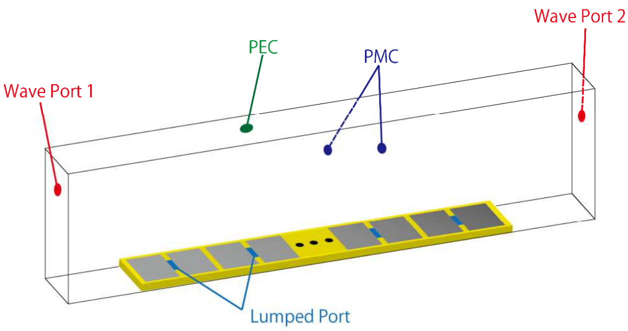

Figure 4. Simulation model deployed inside a TEM waveguide. Patches were connected by one of the circuits drawn in Fig. 3.

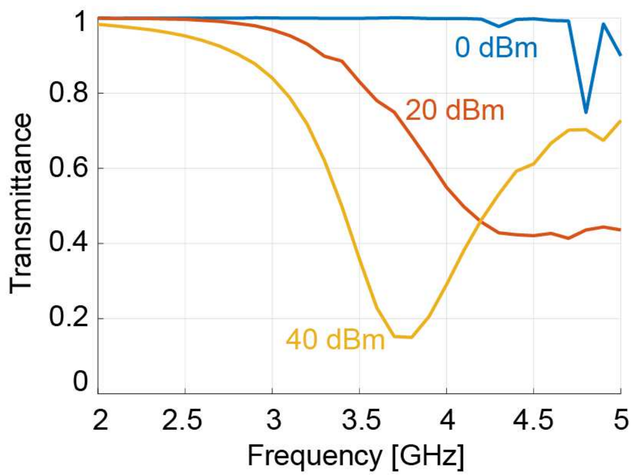

Figure 5. Transmittance of the nonlinear metasurface (see Figs. 3a and 4).

3.3 Anisotropic Waveform-Selective Metasurfaces

Following the design concept of the above nonlinear metasurface, we simulated an anisotropic waveform-selective metasurface inside the same TEM waveguide. In this case, the simulation model was the same as the one used in Fig. 5 except the circuit between conductor edges. The circuit used here is drawn in Fig. 3b, where paired diodes were replaced by a diode bridge as well as an inductor and a resistor. Therefore, the internal inductor exhibited a strong electromotive force to prevent the incoming electric charges in the time domain. In other words, the gap between conductors was connected/disconnected in the time domain depending on the incoming waveform. For instance, Fig. 6 plots the transmittance of the anisotropic waveform-selective metasurface using a short pulse or a continuous wave (CW), both of which had an input power of 30 dBm. As seen in this figure, when the incident waveform was short enough, the metasurface transmitted an incoming wave as conductor edges were not electrically connected due the presence of the electromotive force of inductors. This force, however, decreased when the waveform became sufficiently long so that every two patches were connected to effectively form rectangular patches. As a result, the transmittance was reduced around 5 GHz. These simulation results demonstrate that the proposed structure varies surface impedance depending on the incident waveform, which can potentially be exploited as an anisotropic metasurface. However, we also noticed that the present structure also contained a loss mechanism, which lowered the magnitude of the reflected wave. Therefore, our proposed structure still requires improvement to reduce the loss mechanism.

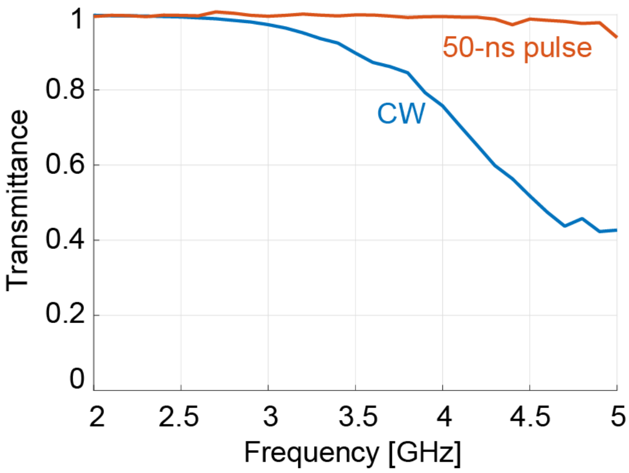

Figure 6. Transmittance of the waveform-selective metasurface (see Figs. 3b and 4).

4 Conclusion

In conclusion, we have reported simulation results of an anisotropic waveform-selective metasurface to realize the guiding of a surface wave for scattering reduction depending on the incoming waveform. Such a new capability is expected to give us a new degree of freedom to address electromagnetic interference issues, while still maintaining antenna communications at the same frequency through use of a particular waveform. In this presentation, we are planning to report more extended results including experimental verification.

4 Acknowledgements

This work was supported in part by the Japanese Ministry of Internal Affairs and Communications (MIC) under Strategic Information and Communications R&D Promotion Program (SCOPE) No. 165106001 and 192106007 and the Japan Science and Technology Agency (JST) under Precursory Research for Embryonic Science and Technology (PRESTO) No. JPMJPR193A.

5 References

1. D. Sievenpiper, L. Zhang, R.F.J. Broas, N.G. Alexopolous, and E. Yablonovitch, "High-Impedance Electromagnetic Surfaces with a Forbidden Frequency Band," *IEEE Trans. Microw. Theory Tech.*, 47, 11, 2059, 1999.

2. N. Yu, P. Genevet, M. A. Kats, F. Aieta, J. P. Tetienne, F. Capasso, and Z. Gaburro, "Light Propagation with Phase Discontinuities: Generalized Laws of Reflection and Refraction," *Science*, 334, 333, 2011.

3. N. Yu and F. Capasso, "Flat Optics with Designer Metasurfaces," *Nat. Mater.*, 13, 139, 2014.

4. R. Quarfoth and D. Sievenpiper, "Artificial Tensor Impedance Surface Waveguides," *IEEE Trans. Antennas Propag.*, 61, 7, 359, 2013.

5. J. Lee and D. Sievenpiper, "Patterning Technique for Generating Arbitrary Anisotropic Impedance Surfaces," *IEEE Trans. Antennas Propag.*, 64, 11, 4725, 2016.

6. J. Lee and D. Sievenpiper, "Method for Extracting the Effective Tensor Surface Impedance Function from Nonuniform, Anisotropic, Conductive Patterns," *IEEE Trans. Antennas Propag.*, 67, 5, 3171, 2019.

7. H. Wakatsuchi, S. Kim, J. J. Rushton, and D. F. Sievenpiper, "Waveform-Dependent Absorbing Metasurfaces," *Phys. Rev. Lett.*, 111, 24, 245501, 2013.

8. H. Wakatsuchi, D. Anzai, J. J. Rushton, F. Gao, S. Kim, and D. F. Sievenpiper, "Waveform Selectivity at the Same Frequency," *Sci. Rep.*, 5, 9639, 2015.

9. H. Wakatsuchi, J. Long, and D. Sievenpiper, "Waveform Selective Surfaces," *Adv. Funct. Mater.*, 29, 11, 1806386, 2019.

10. S. Vellucci, A. Monti, M. Barbuto, A. Toscano, and F. Bilotti, "Waveform-Selective Mantle Cloaks for Intelligent Antennas," *IEEE Trans. Antennas Propag.*, 68, 3, 1717, 2020.

11. M.F. Imani and D.R. Smith, "Temporal Microwave Ghost Imaging Using a Reconfigurable Disordered Cavity," *Appl. Phys. Lett.*, 116, 054102, 2020.

12. K. Asano, T. Nakasha, and H. Wakatsuchi, "Simplified Equivalent Circuit Approach for Designing Time-Domain Responses of Waveform-Selective Metasurfaces," *Appl. Phys. Lett.*, 116, 171603, 2020.